sustainability

MDPI

Article

Quantifying Degradation Classifications on Alpine Grassland in the Lhasa River Basin, Qinghai-Tibetan Plateau

Wangya Han [1,2], Huiting Lu [1,2], Guohua Liu [1,2,*], Jingsheng Wang [3] and Xukun Su [1,2,*]

1 State Key Laboratory of Urban and Regional Ecology, Research Center for Eco-Environmental Sciences, Chinese Academy of Sciences, Beijing 100085, China; wyhan_st@rcees.ac.cn (W.H.); htlu_st@rcees.ac.cn (H.L.)
2 College of Resources and Environment, University of Chinese Academy of Sciences, Beijing 100049, China
3 Key Laboratory of Ecosystem Network Observation and Modeling, Institute of Geographic Sciences and Natural Resources Research, Chinese Academy of Sciences, Beijing 100101, China; wangjsh@igsnrr.ac.cn
* Correspondence: ghliu@rcees.ac.cn (G.L.); xksu@rcees.ac.cn (X.S.)

Received: 21 November 2019; Accepted: 9 December 2019; Published: 10 December 2019

check for updates

Abstract: The Qinghai-Tibetan Plateau (QTP) has the world's largest alpine grassland ecosystem. The QTP ecosystem is extremely fragile and suffers continuous degradation. An accurate determination of the status of alpine grassland is the first crucial step in monitoring its degradation. A novel method combining field survey with remote sensing information based on ecological indicators is proposed. The degradation classification of alpine grassland was identified by multivariate hierarchical analysis based on 270 field plots. The spatial pattern of alpine grassland degradation was mapped by determining remote sensing variables that corresponded to field indicators of the degradation classification system. The results showed that clustering analysis divided the degradation classification of alpine grassland into five classes: Non-Degraded (ND), Slightly Degraded (SLD), Moderately Degraded (MD), Severely Degraded (SD), and Extremely Degraded (ED). The most significant factors for alpine grassland degradation included the dominance of Cyperaceae plants, soil total nitrogen content, soil organic carbon content, soil total carbon content, soil bulk density, soil pH, dominance of miscellaneous plants, and elevation among all 17 variables. The assessment and mapping of alpine grassland degradation provide an important basis for alpine grassland protection and management, particularly at a large scale.

Keywords: alpine grassland; quantitative degradation classifications; remote sensing; Lhasa river basin

1. Introduction

Grassland is an important part of terrestrial ecosystems, with natural vegetation types including steppe, meadow, marsh, tundra, savanna, desert, and woodland [1]. Grassland plays important ecological and socio-economic roles, such as affecting biodiversity by evolving grass species that shape grassland environments [2] and storing carbon as carbon sinks and impacting livestock by producing forage [3]. Grassland degradation manifests in the reduction of grassland productivity, deterioration of the environment, and loss of biodiversity, suffering from natural processes and human activities [4]. Grassland degradation is a global problem as demonstrated by the fact that nearly half of the world's grasslands are degraded [5]. Additionally, 90% of grassland in China has been degraded to some extent [6]. The alpine grassland of the Qinghai-Tibetan Plateau (QTP) has suffered from increasingly severe degradation in recent decades due to livestock over-grazing, rodent damage, and climate changes [3,7]. Herbivore (mainly yaks and sheep) grazing affects the productivity and the function of grassland ecosystems. The alpine grassland of the QTP is one of the most important grazing lands in the world, and it is distributed in the headwaters of Asia's major rivers on which approximately 40% of the world's population depends [8].

Monitoring and preventing grassland degradation require an accurate assessment of the levels of grassland degradation. The first critical step in the assessment of degraded grassland is to determine the pertinent indicators and thresholds of degradation [9,10]. Indicators can reflect and explain changes in ecosystems that result from grassland degradation. Biological indicators and soil indicators are the main indices of grassland degradation, and biological indicators are more commonly used at large scales due to the difficulty of obtaining soil indicators at the regional scale [7]. Ecological thresholds describe when and where the stable states of ecosystem changes. There are no uniform or specific methods to identify the threshold ranges. The selection of different indicators and the definition of threshold ranges must consider stress, which directly affects the results of a degradation assessment.

Multiple methods are used to assess alpine grassland degradation, including field measurements, remote sensing, and non-parametric approaches. Field methods are limited because they require a large workload, have low testing frequency, and are time consuming and expensive [11]. Due to its spatially explicit and temporal dynamic attributes, remote sensing is widely used in monitoring alpine grassland degradation by providing spectral information reflecting vegetation characteristics [4,12,13]. However, the accuracy of vegetation indices is limited, especially when it is affected by soil background values for sparse grasslands [14,15]. Non-parametric approaches are especially suitable for the incorporation of non-spectral data for supplementing degraded classification based only on spectral information [16], including neural networks, knowledge-based approaches and decision trees. The neural network has the capacity for self-learning, self-adaptation, and high fault tolerance, but the preprocessing of data and network structure will affect the function of the neural network [16,17]. The knowledge-based approach can accommodate multiple data sources, improving the classification accuracy to some extent [10]. However, the classification is easily influenced by subjective factors. The decision tree is flexible and intuitive and has high operational efficiency [17]. The degree of degraded alpine grassland varies with different assessment methods based on the different classification systems. In contrast, qualitative classification approaches are widely used in studies of grassland degradation [18,19], and quantitative approaches have been used in some areas of the world [20,21], though rarely on the QTP.

This study presents a quantitative classification method based on decision tree using field data, and this proposed method improves the accuracy of remote sensing assessments of alpine grassland degradation by combining topography and soil type data. Our objectives were to (i) determine the thresholds of key indicators to quantify degradation classification, (ii) obtain the distribution pattern of alpine grassland degradation at the regional scale, and (iii) propose targeted alpine grassland management measures based on different degrees of degradation.

2. Materials and Methods

2.1. Study Area

The Lhasa River basin is located in the southern QTP (90°05′–93°20′ E, 29°20′–31°15′ N) and has an area of 3.26×10^4 km^2 (Figure 1). The terrain declines in altitude from north to south, and the elevation ranges from 3598 m to 7074 m, with geographical characteristics of mountains and valley plains. The study area is within the plateau temperate semi-arid monsoon climate zone. The mean annual temperature ranges from −7.1 °C to 9.2 °C, and the multiyear average precipitation ranges from 340 mm to 700 mm. The vegetation types mainly include alpine meadow, alpine steppe, mountain shrub grassland, shrub, and sparse mountain forest [22]. The soil types are mainly leptosols, cambisols, gleysols, and phaeozems. This area has suffered from severe grassland degradation due to the long-term lack of scientific management and the under-developed utilization pattern of grassland resources, which includes over-grazing and rodent damage. The alpine grassland ecosystem has been destroyed and sustainable development of alpine grassland livestock husbandry has been restricted.

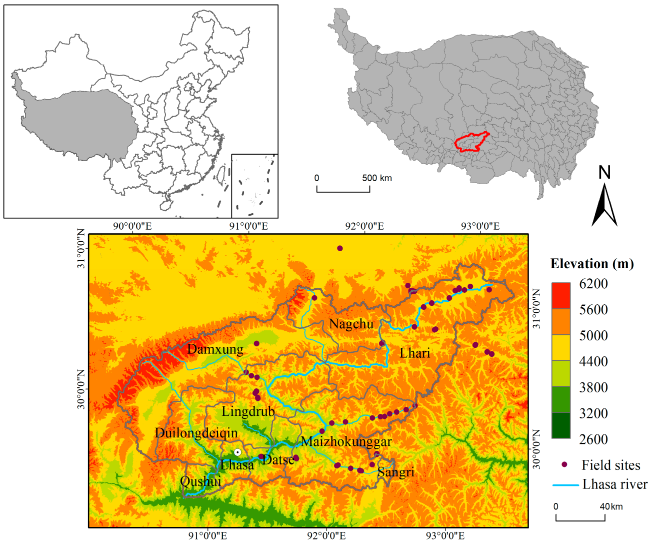

Figure 1. Location of the study area.

2.2. Field Data

We selected 64 field sites of representative alpine grassland that covered all types of alpine grassland in the study area. Five subsites representing "Non-Degraded" (ND), "Slightly Degraded" (SLD), "Moderately Degraded" (MD), "Severely Degraded" (SD), and "Extremely Degraded" (ED) alpine grassland were designated at each site in reference to the alpine grassland coverage described by Wang et al. [23]. One plot (1 m × 1 m) was set randomly in each subsite, and the plots were separated by at least 10 m buffer. Twenty-four sites did not have five subsites (22 of them had three subsites, and two had two subsites), yielding a total of 270 plots across the region.

All field data were measured during the growing season between July and August in 2017. The latitude, longitude, and elevation of the subsites were recorded by a Global Positioning System (GARMIN GPSMAP® 631sc). The slope and aspect were measured using an inclinometer and a compass. In each plot, vegetation parameters were measured, including total vegetation coverage, bare land coverage, species richness, coverage of each species, height of each species, and dominance of plant functional groups. The total vegetation coverage and bare land coverage were calculated by fisheye lens images. Species richness was simply the total number of species per plot. The coverage of each species was calculated from the number of individuals of each one. The height of each species was calculated as the average from five random individuals. The plant groups in plots were apportioned into four functional groups containing Cyperaceae plants, Poaceae plants, miscellaneous plants, and inedible plants [24]. The dominance index is based on Importance Values (IVs) of species, and the proportion of the total IVs was calculated as follows [25]:

$$p_i = \frac{\left(\frac{C_i}{\sum_i^S C_i} + \frac{H_i}{\sum_i^S H_i} + \frac{F_i}{\sum_i^S F_i}\right)}{3} \times 100 \tag{1}$$

where p_i is the important value in the plot, S is the total number of species, C_i is the coverage of species i, H_i is the height of species i, and F_i is the frequency of species i.

Soil samples (0–20 cm depth) were collected in each plot and used for measurements of the soil moisture content, soil bulk density, soil pH, soil total carbon, soil organic carbon, soil total nitrogen, soil available nitrogen, soil available phosphorus, and soil available potassium. The soil moisture content and soil bulk density were determined by the oven drying method, according to

Thomasson [26]. The soil pH was measured on a 1:1 water/soil suspension using a pH meter [27]. Soil total carbon and soil total nitrogen were measured using the flash dynamic combustion method, gas chromatographic separation, and thermal conductivity detection system (vario EL cube Elementar, Germany), respectively [28]. Soil organic carbon was determined by the dichromate oxidation method [29]. Soil available nitrogen was measured using the alkali-hydrolysis reduction diffusion method [30,31]. Soil available phosphorus was extracted with the ammonium bicarbonate method, and soil available potassium was extracted using the acetamide extraction method [32].

2.3. Remote Sensing Data

Landsat 8 OLI satellite images were acquired on 10 July 2017, corresponding to the field survey time as much as possible under the condition of no clouds. Eight Landsat 8 images (path/row number: 138/038, 138/039, 138/040, 137/038, 137/039, 137/040, 136/038, 136/039) were downloaded from the United States Geological Survey (USGS) website (http://earthexplorer.usgs.gov) at a spatial resolution of 30 m. These images were processed by radiance calibration and atmospheric correction in ENVI 5.1. In this study, we used only two bands: Band 4 (636–673 nm) and Band 5 (851–879 nm). The vegetation indices considered in this case, including the normalized difference vegetation index (NDVI), soil adjusted vegetation index (SAVI), and renormalized difference vegetation index (RDVI) (according to Davidson et al.) were calculated as follows:

$$\mathrm{NDVI} = \frac{NIR - R}{NIR + R} \tag{2}$$

$$\mathrm{SAVI} = \frac{(NIR - R)(1 + L)}{(NIR + R + L)} \tag{3}$$

$$\mathrm{RDVI} = \frac{NIR - R}{\sqrt{NIR + R}} \tag{4}$$

where NIR is the radiance in the near infrared region band (NIR = Band5), R is the radiance in red band (R = Band 4), and L is the soil correction factor. In this study, the L value equals 0.5 [33].

The elevation data were derived from ASTER Global DEM (GDEM) with a spatial resolution of 30 m (http://srtm.csi.cgiar.org). The soil type was derived from spatial distribution data of soil types in China at a scale of 1/1000000 (http://www.resdc.cn). The coverage map of bare land was derived from the MOD44B Version 6 Vegetation Continuous Fields (VCF) product with a spatial resolution of 250 m (https://lpdaac.usgs.gov/dataset_discovery/modis/modis_products_table/mod44b_v006).

2.4. Statistical Analysis

All statistical analyses were performed in R version 3.5.0 with the Vegan and the Rpart libraries [34]. Euclidean distance matrices were used for community dissimilarity analysis, and hierarchical clustering using Ward's method was calculated on this basis [35]. Nonmetric multidimensional scaling (NMDS) analysis was used to test the differences in plant community composition among different degraded levels of alpine grassland. The "envfit" function software package was used to determine which biophysical variables correlated well with ordination space. Seventeen field-derived biophysical variables were selected and normalized to range from zero (0) to one (1) (Table 1). The main factors affecting the ordination were chosen by excluding collinear factors. Classification and regression tree (CART) analysis was used to characterize the main biophysical factors of subsites classified as ND, SLD, MD, SD, and ED. The tree determined the thresholds of variables by encoding a set of decision rules in the form of if-then statements [20]. The CART model was pruned by reducing its size to the minimum of the cross-validation error [36].

Table 1. Biophysical variables used in the analysis.

Type of Variable	Variable	Unit	Range of Values
Biotic	Total vegetation cover	%	5–100
	Dominance of Cyperaceae plants	%	0–77.61
	Dominance of Poaceae plants	%	0–52
	Dominance of inedible plants	%	0–72.48
	Dominance of miscellaneous plants	%	0–72.48
Abiotic	Bare land cover	%	13–67
	Soil moisture content	%	0.18–135.20
	Soil bulk density		0.33–1.69
	Soil pH		0.34–8.26
	Soil total carbon content	%	0.3–20.29
	Soil total nitrogen content	%	0.09–6.21
	Soil organic carbon content	%	0.60–18.72
	Soil available nitrogen content	mg kg^{-1}	3–1102.5
	Soil available phosphorus content	mg kg^{-1}	0.36–908
	Soil available potassium content	mg kg^{-1}	4.2–637.5
Topographic	Elevation	m	3700–5368
	Slope	degree	0.75–45

2.5. Spatial Pattern of Alpine Grassland Degradation

Based on the main factors of alpine grassland degradation determined by multivariate statistical analysis, the corresponding GIS layers were selected (Table 2). Among them, the NDVI, SAVI, and RDVI were chosen as vegetation index layers because of their suitability for alpine grassland degradation according to Zha [4]. The indicator thresholds of alpine grassland degradation obtained by CART analysis consummated the degradation classifications at the field scale. The sites with different degradation classes were placed on the GIS layers, and the pixel values of the sites in each layer were extracted. Thus, the ranges of the pixel values of each layer in the different degradation classes were obtained. The grading layers were in accordance with the locations of the plots in the different classes in layers. We divided the degradation class of alpine grassland according to the values ranging from low (1) to high (5). The most frequent score was the overall assessment score of degradation at each pixel scale (Figure 2).

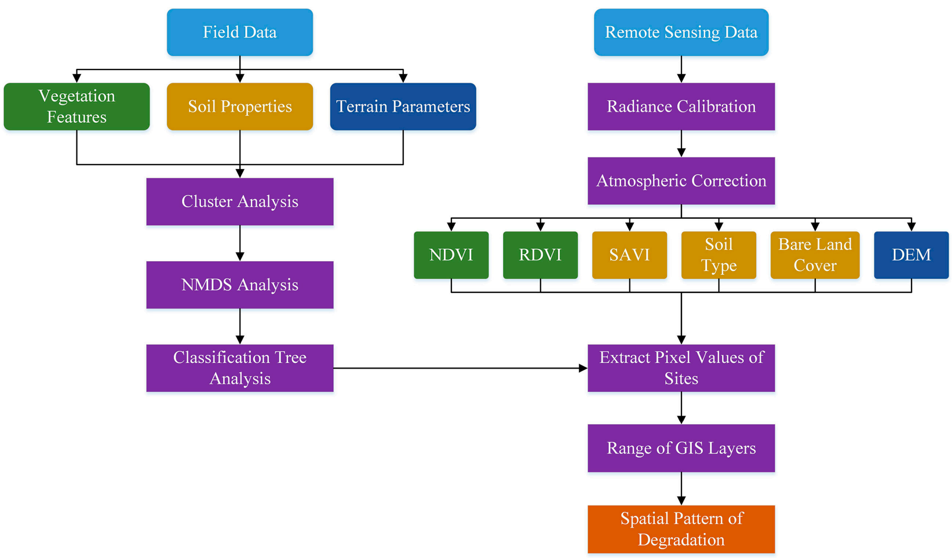

Figure 2. Process of quantitative degradation classification.

Table 2. Criteria of degradation classification for alpine grassland in GIS layers.

Degradation Level	Score	NDVI	SAVI	RDVI	Bare Land Cover (%)	Elevation (m)	Soil Type
ND	1	>0.30	>0.27	12.44–15.00	<37	4130–4200	Dark felty soils
SLD	2	0.27–0.30	0.20–0.27	9.44–12.44	37–40	4950–5110	Swamp soil, Alpine frost soil
MD	3	0.24–0.27	0.14–0.20	>15.00	40–46.5	4200–4500, 4700–4950, >5110	Felty soils, Meadow soil
SD	4	0.08–0.24	0.05–0.14	5.73–9.44	46.5–55	3720–4130, 4500–4700	Frigid calcic soils
ED	5	<0.08	<0.05	<5.73	>55	<3720	Cold brown calcic soils

Note: ND: Non-Degraded, SLD: Slightly Degraded, MD: Moderately Degraded, SD: Severely Degraded, ED: Extremely Degraded.

3. Results

3.1. Classification of Subsites to Identify Degradation Classes

The cluster analysis showed that the 270 plots could be classified into five groups (Figure 3). They include Cluster 2, Cluster 5, Cluster 4, Cluster 3, and Cluster 1, represented the ND, SLD, MD, SD, and ED classes of alpine grassland degradation, respectively. Significant differences in the biophysical variables were found among the different degradation classes (Table 3). The total vegetation coverage of SLD and MD decreased by 9.31% and 13.35%, respectively, compared with that of ND. SD and ED showed significantly decreased total vegetation coverage by 36.84% and 70.69%, respectively, relative to ND. Compared with ND, SLD and MD exhibited significantly increased dominance of Cyperaceae plants by 137.73% and 101.64%. However, the dominance of Cyperaceae plants in SD and ED was lower by 26.89% and 61.21% compared with that in ND, and significantly lower by 69.25% and 83.68% compared with that in SLD. ND and SLD showed no significant difference in the dominance of Poaceae plants, but MD, SD, and ED increased by 14.88%, 116.38%, and 369.74% compared with SLD, while ED exhibited a significant increase. The dominance of inedible plants exhibited a similar trend to the dominance of Poaceae plants in different degradation classes. The dominance of miscellaneous plants in SLD and MD was significantly lower than that of ND by 42.06% and 41.02%, respectively. Bare land cover showed an increasing trend with increasing degradation level as a whole, and the bare land cover was significantly increased in ED compared with ND, SLD, MD, and SD. The soil water content, soil total carbon content, soil organic carbon content, soil total nitrogen content, soil available nitrogen content, and soil available potassium content decreased with increasing degradation level, while the soil total carbon content exhibited a significant decrease. The soil bulk density and soil pH increased with the aggravation of alpine grassland degradation. The soil available phosphorus content was not significantly different in the different degradation classes. The changes in elevation and slope were not highly significant. Consequently, the subsites can be classified into different clusters through a statistical analysis method based on the biophysical variables.

Table 3. Descriptive statistics for biophysical variables of different classes of degradation.

Variable	ND		SLD		MD		SD		ED		P	F
	Mean ± SD	**CV%**	**Mean ± SD**	**CV%**	**Mean ± SD**	**CV%**	**Mean ± SD**	**CV%**	**Mean ± SD**	**CV%**		
Total Vegetation cover (%)	83.17 ± 15.27 ^{a}	18.36	75.42 ± 23.31 ^{a}	30.90	72.06 ± 24.74 ^{a}	34.33	52.53 ± 26.69 ^{b}	50.81	24.38 ± 7.03 ^{c}	28.86	<0.01	17.775
Dominance of Cyperaceae Plants (%)	19.66 ± 0.05 ^{c}	0.28	46.73 ± 0.09 ^{a}	0.18	39.64 ± 0.11 ^{b}	0.28	14.37 ± 0.12 ^{c}	0.84	7.62 ± 0.10 ^{c}	1.30	<0.01	79.82
Dominance of Poaceae Plants (%)	7.20 ± 0.05 ^{b}	0.73	5.10 ± 0.06 ^{b}	1.21	5.86 ± 0.07 ^{b}	1.22	11.04 ± 0.11 ^{b}	1.03	23.98 ± 0.06 ^{a}	0.26	<0.01	13.459
Dominance of inedible Plants (%)	20.80 ± 0.08 ^{cd}	0.41	17.84 ± 0.07 ^{d}	0.41	23.63 ± 0.11 ^{c}	0.46	30.73 ± 0.16 ^{b}	0.51	54.40 ± 0.11 ^{a}	0.21	<0.01	21.928
Dominance of miscellaneous Plants (%)	52.34 ± 0.06 ^{a}	0.12	30.32 ± 0.08 ^{b}	0.28	30.87 ± 0.11 ^{b}	0.35	43.86 ± 0.16 ^{a}	0.36	14.00 ± 0.06 ^{c}	0.40	<0.01	26.981
Bare Land Cover (%)	40.67 ± 4.47 ^{bc}	11.00	36.04 ± 11.62 ^{c}	32.25	39.32 ± 13.02 ^{bc}	33.10	42.19 ± 11.56 ^{b}	27.40	55.38 ± 0.48 ^{a}	0.87	<0.01	5.773
Soil Moisture Content (%)	50.95 ± 19.54 ^{a}	38.34	53.22 ± 23.65 ^{a}	44.43	48.75 ± 27.20 ^{a}	55.80	29.31 ± 28.24 ^{b}	96.35	8.79 ± 4.03 ^{b}	45.81	<0.01	12.549
Soil Bulk Density	0.70 ± 0.17 ^{bc}	24.74	0.77 ± 0.19 ^{c}	24.42	0.81 ± 0.24 ^{bc}	29.99	1.06 ± 0.27 ^{b}	25.52	1.51 ± 0.07 ^{a}	4.96	<0.01	12.063
Soil pH	5.78 ± 0.26 ^{c}	4.42	5.63 ± 0.41 ^{c}	7.32	5.76 ± 0.75 ^{c}	13.04	6.36 ± 0.77 ^{b}	12.08	8.04 ± 0.30 ^{a}	3.76	<0.01	24.683
Soil Total Carbon Content (%)	7.35 ± 2.69 ^{a}	36.63	6.94 ± 3.73 ^{b}	53.68	5.22 ± 1.96 ^{c}	37.54	4.51 ± 3.18 ^{c}	70.50	0.82 ± 0.08 ^{d}	10.00	<0.01	13.246
Soil Total Nitrogen Content (%)	0.59 ± 0.20 ^{a}	33.55	0.55 ± 0.26 ^{a}	46.56	0.42 ± 0.13 ^{b}	31.43	0.40 ± 0.25 ^{b}	62.02	0.11 ± 0.01 ^{b}	13.26	<0.01	7.726
Soil Organic Carbon Content (%)	6.86 ± 2.82 ^{a}	41.12	6.87 ± 3.64 ^{a}	53.06	5.14 ± 1.96 ^{b}	38.19	4.45 ± 3.08 ^{b}	69.29	0.78 ± 0.10 ^{c}	12.64	<0.01	12.389
Soil Available Nitrogen Content (mg kg^{-1})	578.66 ± 237.09 ^{a}	40.97	509.69 ± 93.43 ^{a}	18.33	449.80 ± 169.09 ^{ab}	37.59	369.16 ± 266.57 ^{b}	72.21	57.15 ± 27.33 ^{c}	47.82	<0.01	12.095
Soil Available Phosphorus Content (mg kg^{-1})	8.65 ± 5.34 ^{a}	61.70	7.37 ± 2.57 ^{a}	34.90	14.58 ± 86.04 ^{a}	590.03	7.41 ± 6.38 ^{a}	86.13	1.48 ± 0.69 ^{a}	46.65	0.87	0.307
Soil Available Potassium Content (mg kg^{-1})	214.47 ± 117.47 ^{a}	54.77	177.59 ± 93.43 ^{ab}	52.61	163.87 ± 88.49 ^{ab}	54.00	146.46 ± 67.75 ^{b}	46.26	96.31 ± 39.61 ^{b}	41.12	<0.01	3.914
Elevation (m)	4416.06 ± 245.56 ^{b}	5.56	4801.97 ± 284.65 ^{a}	5.93	4693.73 ± 306.99 ^{a}	6.54	4479.46 ± 413.53 ^{b}	9.23	4256.88 ± 431.35 ^{b}	10.13	<0.01	12.52
Slope (degree)	14.41 ± 3.55 ^{ab}	24.61	10.14 ± 9.44 ^{b}	93.08	11.12 ± 10.15 ^{b}	91.30	15.37 ± 10.74 ^{a}	69.89	4.77 ± 0.29 ^{b}	6.15	<0.01	4.413

Note: ND: Non-Degraded, SLD: Slightly Degraded, MD: Moderately Degraded, SD: Severely Degraded, ED: Extremely Degraded.

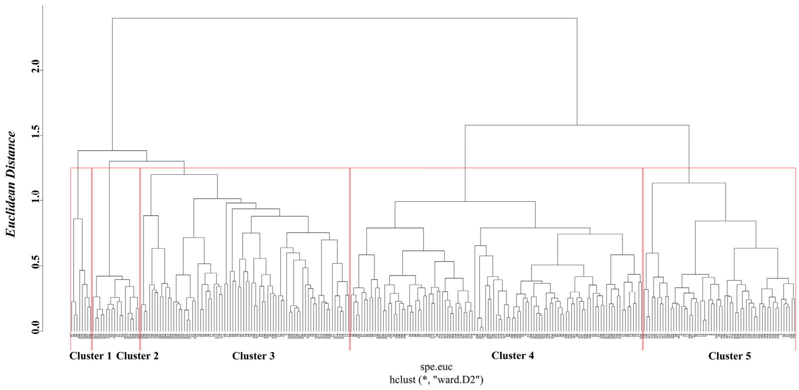

Figure 3. Degradation classification by cluster analysis based on 17 field-derived biophysical variables.

3.2. Main Biophysical Factors of Classified Subsites

The NMDS analysis showed the ordination space of all subsites clustered based on the degree of alpine grassland degradation (Figure 4). The goodness-of-fit of the ordination in linear regression and non-linear regression was high with R^2 values of 0.958 and 0.871, respectively. All the variables were correlated with the ordination pattern of the subsites, with the exception of the soil available phosphorus content and soil available potassium content. Different variables did not have the same influence on the subsite ordination. The subsites plotted toward the ND class were correlated with elevation. SLD and MD were correlated with the dominance of Cyperaceae plants, total vegetation coverage, soil water content, soil total carbon content, soil total nitrogen content, soil organic carbon content, and soil available nitrogen content. These two classes showed the highest correlation with the dominance of Cyperaceae plants. SD and ED were correlated with the dominance of inedible plants, dominance of Poaceae plants, dominance of miscellaneous plants, soil bulk density, soil pH, bare land cover, and slope. They were highly correlated with the dominance of inedible plants, dominance of Poaceae plants, soil bulk density, and soil pH. Collinear variables were found among all of these variables. Bare land cover had significant collinearity with slope. Soil available phosphorus content and soil available potassium content were strongly collinear. Considering collinearity and weak correlations, the main biophysical factors of the classified subsites included all variables except slope, soil available phosphorus content, and soil available potassium content.

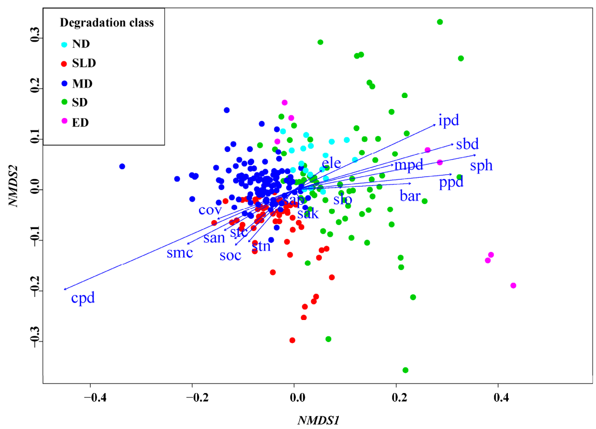

Figure 4. Nonmetric multidimensional scaling analyses for five degradation classes. ele: elevation, slo: slope, cov: total vegetation cover, cpd: dominance of Cyperaceae plants, ppd: dominance of Poaceae plants, ipd: dominance of inedible plants, mpd: dominance of miscellaneous plants, smc: soil moisture, sbd: soil bulk density, sph: soil pH, stn: soil total nitrogen content, stc: soil total carbon content, soc: soil organic carbon content, san: soil available nitrogen content, sap: soil available phosphorus content, and sak: soil available potassium content.

3.3. Thresholds of Variables Affecting Degradation

A pruned classification tree can encode a set of decision rules to predict the classification of five degraded alpine grassland types, which can be used to determine the main predictor variables and their thresholds (Figure 5). For example, the right most decision rule can be translated as follows: "when the dominance of Cyperaceae plants is greater than 27.85% and the soil organic carbon content is less than 0.88%, seven subsites were classified as extremely degraded". Figure 5 shows that the main predictor variables included the dominance of Cyperaceae plants, soil total nitrogen content, soil organic carbon content, soil total carbon content, soil bulk density, soil pH, dominance of miscellaneous plants, and elevation, as noncollinear variables with relatively strong effects in the NMDS analysis. The thresholds determined by the classification tree partitioned the degradation classes, obtaining quantitative grading criteria of alpine grassland degradation.

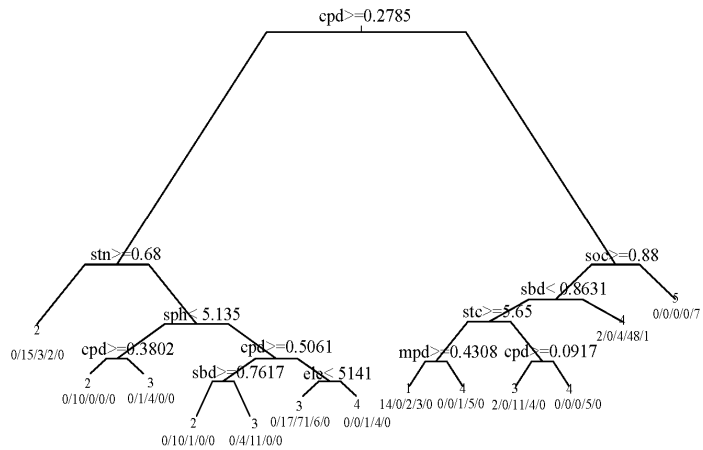

Figure 5. Classification tree analysis of five degraded alpine grassland types. The numbers 1 to 5 represent Cluster 1 to Cluster 5, respectively.

3.4. Spatial Pattern of Alpine Grassland Degradation

Figure 6 shows the spatial pattern of alpine grassland degradation obtained from quantitative classification based on both fieldwork and remote sensing data. The grassland with an area of 2.26×10^4 km^2 was divided into five levels. The criteria for alpine grassland degradation are presented in Table 2. Of the alpine grassland area, 4.34% was classified as ND, 2.52% as SLD, 49.30% as MD, 27.79% as SD, and 16.06% as ED. The ND was mainly located in the valley of Maizhokunggar County, which is in the southeastern region of the Lhasa River basin, comprising 14.20% of the area. The SD of alpine grassland comprised 5.00% and was found in the Medica wetlands in northeastern Lhari County. The MD was widely distributed throughout the entire basin, occupying 62.36% of Datse, 58.08% of Qushui, 55.64% of Chengguan District of Lhasa city, 52.64% of Damxung, 52.53% of Duilongdeiqin, 50.36% of Nagchu, 47.56% of Sangri, 46.19% of Maizhokunggar, and 42.17% of Lhari. In the county of Lingdrub in this basin, 35.99% of the area was classified as SD, followed by Damxung County, where the severe class occupied 34.08%. The ED of alpine grassland degradation was scattered in the study area, in which Lhari and Maizhokunggar counties had larger proportions of 29.90% and 17.39%, respectively.

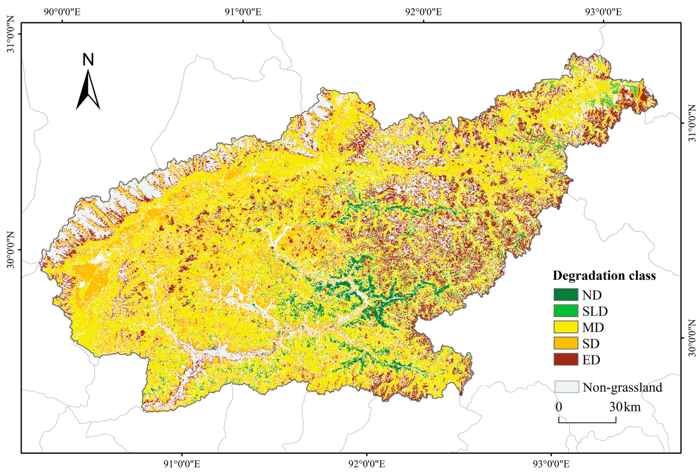

Figure 6. Distribution pattern of alpine grassland degradation in the Lhasa River basin.

4. Discussion

4.1. Validity of the Classification Method for Alpine Grassland Degradation

The NMDS is an unconstrained ordination analysis based on any type of distance matrix. Bray-Curtis dissimilarity matrices are commonly used in NMDS ordination [37]. For this multivariate statistical method based on distance matrices, the selection of an appropriate distance matrix directly affects the rationality of the results [38]. In this study, the cophenetic correlation coefficients of the clustering model were compared, and the results showed that the Euclidean distance had a value of 0.72 and a Bray-Curtis distance of 0.58. Thus, the Euclidean distance has a better clustering effect than the Bray-Curtis distance. The Euclidean distance was used in NMDS ordination [9] when it was more robust than Bray-Curtis.

The vegetation index (VI) is the result of an arithmetic operation between the pixel values of two or more spectral bands, which are correlated with plant parameters [39,40], and reveals the status of grassland degradation. The appropriate VIs of the QTP included NDVI, SAVI, and RDVI, which were selected by univariate linear regression analysis, with the larger R^2 values including the percent grass cover and the proportion of unpalatable grass as dependent variables [4]. NDVI is widely used for monitoring natural biological communities and agricultural ecosystems due to its easy accessibility and commonality. However, for sparse vegetation, the soil background contributes greatly to the total spectral reflectance [14], and it is not appropriate to evaluate grassland degradation using only NDVI. SAVI was proposed to compensate for the corresponding soil effect, reducing the significant contribution of soil reflectivity [41]. In high vegetation cover areas, NDVI is easily saturated, and RDVI can avoid the problems applied in the cases of high and low vegetation coverage, thus better adapting to areas with large disparities in coverage [42].

4.2. Quantitative Classifications of Alpine Grassland Degradation

The assessment of grassland degradation states is an important prerequisite for restoring and treating degraded grassland. Quantitative classifications of degradation can represent the degradation states more accurately. Alpine grasslands with different classes of degradation require different corresponding restoration and management measures [43], and the quantitative grading of degradation contributes to a more scientific alpine grassland management. The ecological thresholds of indicators in degradation assessment provide guidance for management thresholds and have theoretical and practical value for the scientific management of alpine grassland ecosystems [9]. Compared with field surveys, remote sensing is widely used in large-scale grassland degradation because of its higher efficiency [4,44,45], but quantitative classifications at a larger scale are rare in assessment studies.

In this study, the quantitative degradation classifications reflected the spatial pattern of grassland degradation on the basis of field data processed by multivariate statistical analysis.

4.3. Analysis of Different Classes of Grassland Degradation Combined with Management Measures

The distribution patterns of grassland degradation have spatial heterogeneity affected by different natural and human factors. The ND areas were mainly distributed in western Maizhokunggar County because this area is characterized by montane shrub grassland with a relatively low level of human activities such as grazing and farming. Most of the SLD areas were located in eastern Lhari County of the study area, and the vegetation type is composed mainly of wetland with a swamp soil. The MD areas were widely distributed in the study area, concentrated in Damxung and Lhari County. Grazing livestock is a heavy attribute for high forage quality with the vegetation types of alpine meadow, temperate grassland and alpine grassland and at higher altitudes. For SD areas, 27% was located in Damxung and 19% in Lingdrub. Sparse grassland was the main vegetation type, and the elevation was low in this area. With the addition of frequent cultivation activities in the surrounding areas, this area suffered from severe human disturbance. The ED areas were distributed sporadically in the study area, and Lhari County had the largest area. Vegetation coverage was low and bare land area was large, with an NDVI value less than 0.08. The soil types were swamp soil and frozen soil.

For different degradation states, specific measures should be implemented and appropriate restoration measures can improve the effectiveness of rangeland restoration [46]. The ranges of indicator thresholds provide a reference for the specific management threshold under different degradation levels. Once the dominance of Cyperaceae plants exceeds 28%, rangeland can be considered slightly degraded or moderately degraded. Enclosure and fencing are needed to maintain the state of rangeland to prevent it from being more seriously degraded. Rangeland can be regarded as extremely degraded when the dominance of Cyperaceae plants is under 28% and the soil total carbon content is under 0.88%. Certain management practices for rangeland restoration are required, including fencing protection, fertilization, and compensatory seed planting. Once the dominance of Cyperaceae plants is under 28%, soil total carbon content exceeds 0.88% and soil bulk density exceeds 0.86, rangeland can be considered severely degraded. Returning reclaimed land to grasslands should be implemented to reduce the human disturbance caused by frequent cultivated land activities [47].

5. Conclusions

In this study, a quantitative classification of alpine grassland degradation was obtained by a multivariate hierarchical analysis based on field data. Combined with remote sensing information, the scaling classification of degradation from the sample plots scale to the region scale and the spatial pattern of alpine grassland degradation was acquired for the study area. The indicator thresholds of degradation were determined, which contribute to the proceeding of alpine grassland restoration and management measures. The moderately degraded of alpine grassland is the main type (approximately 50%) among the five degradation classes of alpine grassland, and moderately degraded is widely distributed in the study area. When the dominance of Cyperaceae plants is under 28% and the soil total carbon content is under 0.88%, alpine grassland can be considered extremely degraded, and extremely degraded grasslands were found to represent 16% of all alpine grassland. This study not only quantitatively evaluated the degradation situation in this region, but also confirmed the main degradation factors and their corresponding thresholds, which has important significance for pasture production and grazing management.

Author Contributions: W.H. carried out experiments and wrote the manuscript; G.L. and X.S. designed experiments; H.L. analyzed experimental results; W.H. and H.L. investigated sample sites; J.W. designed survey lines; G.L. and X.S. participated in the discussion and gave unique insights on the results.

Funding: This research was supported by the National Key Research and Development Program of China (2016YFC0502102) and the Key Science and Technology Plan of Tibet Autonomous Region (Z2016C01G01/08). The authors declare that they have no conflicts of interest.

Acknowledgments: The authors thank all those who helped us complete this research. We thank all students from the Institute of Remote Sensing and Digital Earth of the Chinese Academy of Sciences and Renmin University of China for helping us survey alpine grassland in the field. Great appreciation also goes to the editorial board and the reviewers of this paper.

Conflicts of Interest: There is no conflict of interest in this manuscript. I would like to declare on behalf of my co-authors that the work described was original research, and it has not been published previously, and not under consideration for publication elsewhere. All the authors listed have approved the manuscript that is enclosed.

References

1. Li, X.L.; Gao, J.; Brierley, G.; Qiao, Y.M.; Zhang, J.; Yang, Y.W. Rangeland degradation on the Qinghai-Tibet plateau: Implications for rehabilitation. *Land Degrad. Dev.* **2013**, *24*, 72–80. [CrossRef]
2. Gieselman, T.M.; Hodges, K.E.; Vellend, M. Human-induced edges alter grassland community composition. *Biol. Conserv.* **2013**, *158*, 384–392. [CrossRef]
3. Harris, R.B. Rangeland degradation on the Qinghai-Tibetan plateau: A review of the evidence of its magnitude and causes. *J. Arid Environ.* **2010**, *74*, 1–12. [CrossRef]
4. Zha, Y. Assessment of grassland degradation near Lake Qinghai, West China, using Landsat TM and reflectance spectra data. *Int. J. Remote Sens.* **2004**, *25*, 4177–4189.
5. Gang, C.; Zhou, W.; Chen, Y.; Wang, Z.; Sun, Z.; Li, J.; Qi, J.; Odeh, I. Quantitative assessment of the contributions of climate change and human activities on global grassland degradation. *Environ. Earth Sci.* **2014**, *72*, 4273–4282. [CrossRef]
6. Nan, Z. The grassland farming system and sustainable agricultural development in China. *Grassl. Sci.* **2010**, *51*, 15–19. [CrossRef]
7. Ru, A.; Wang, H.L.; Feng, X.Z.; Hong, W.; Zhe, W.; Ying, W.; Shen, X.J.; Lu, C.H.; Quaye-Ballard, J.A.; Chen, Y.H.; et al. Monitoring rangeland degradation using a novel local NPP scaling based scheme over the "Three-River Headwaters" region, hinterland of the Qinghai-Tibetan Plateau. *Quat. Int.* **2017**, *444*, 97–114.
8. Foggin, J.M. Depopulating the Tibetan Grasslands: National Policies and Perspectives for the Future of Tibetan Herders in Qinghai Province, China. *Mt. Res. Dev.* **2008**, *28*, 26–31. [CrossRef]
9. Li, X.L.; Perry, G.L.W.; Brierley, G.; Sun, H.Q.; Li, C.H.; Lu, G.X. Quantitative assessment of degradation classifications for degraded alpine meadows (Heitutan), Sanjiangyuan, western China. *Land Degrad. Dev.* **2015**, *25*, 417–427. [CrossRef]
10. Mahyou, H.; Tychon, B.; Balaghi, R.; Louhaichi, M.; Mimouni, J. A Knowledge-Based Approach for Mapping Land Degradation in the Arid Rangelands of North Africa. *Land Degrad. Dev.* **2016**, *27*, 1574–1585. [CrossRef]
11. Boschetti, M.; Bocchi, S.; Brivio, P.A. Assessment of pasture production in the Italian Alps using spectrometric and remote sensing information. *Agric. Ecosyst. Environ.* **2007**, *118*, 267–272. [CrossRef]
12. Prince, S.D.; De Colstoun, E.B.; Kravitz, L. Evidence from rain-use efficiencies does not indicate extensive Sahelian desertification. *Glob. Chang. Biol.* **1998**, *4*, 359–374. [CrossRef]
13. Wu, C. Use of a vegetation index model to estimate gross primary production in open grassland. *J. Appl. Remote Sens.* **2012**, *6*, 063532. [CrossRef]
14. Escribano, P.; Palacios-Orueta, A.; Oyonarte, C.; Chabrillat, S. Spectral properties and sources of variability of ecosystem components in a Mediterranean semiarid environment. *J. Arid Environ.* **2010**, *74*, 1041–1051. [CrossRef]
15. Kennedy, P.J. Monitoring the phenology of Tunisian grazing lands. *Int. J. Remote Sens.* **1989**, *10*, 835–845. [CrossRef]
16. Lu, D.; Weng, Q. A survey of image classification methods and techniques for improving classification performance. *Int. J. Remote Sens.* **2007**, *28*, 823–870. [CrossRef]
17. Xu, E.Q.; Zhang, H.Q.; Li, M.X. Object-Based Mapping of Karst Rocky Desertification using a Support Vector Machine. *Land Degrad. Dev.* **2015**, *26*, 158–167. [CrossRef]
18. Gao, Q.Z.; Wan, Y.F.; Xu, H.M.; Li, Y.; Jiangcun, W.Z.; Borjigidai, A. Alpine grassland degradation index and its response to recent climate variability in Northern Tibet, China. *Quat. Int.* **2010**, *226*, 143–150. [CrossRef]
19. Yang, J.; Ding, Y.; Chen, R. Spatial and temporal of variations of alpine vegetation cover in the source regions of the Yangtze and Yellow Rivers of the Tibetan Plateau from 1982 to 2001. *Environ. Geol.* **2006**, *50*, 313–322. [CrossRef]

20. Gellrich, M.; Baur, P.; Robinson, B.H.; Bebi, P. Combining classification tree analyses with interviews to study why sub-alpine grasslands sometimes revert to forest: A case study from the Swiss Alps. *Agric. Syst.* **2008**, *96*, 124–138. [CrossRef]
21. Miller, J.; Franklin, J. Modeling the distribution of four vegetation alliances using generalized linear models and classification trees with spatial dependence. *Ecol. Model.* **2002**, *157*, 227–247. [CrossRef]
22. Gong, T.; Liu, C.; Liu, J. Hydrological Response of Lhasa River to Climate Change and Permafrost Degradation in Xizang. *Acta Geogr. Sin.* **2006**, *61*, 519–526.
23. Wang, J.; Wang, G.; Hu, H.; Wu, Q. The influence of degradation of the swamp and alpine meadows on CH4 and CO2 fluxes on the Qinghai-Tibetan Plateau. *Environ. Earth Sci.* **2010**, *60*, 537–548. [CrossRef]
24. Shang, Z.H.; Ma, Y.S.; Long, R.J.; Ding, L.M. Effect of fencing, artificial seeding and abandonment on vegetation composition and dynamics of 'black soil land' in the headwaters of the Yangtze and the Yellow Rivers of the Qinghai-Tibetan Plateau. *Land Degrad. Dev.* **2010**, *19*, 554–563. [CrossRef]
25. Wang, Y.S.; Shangguan, T.L. Discussion on Calculating Method of Important Values. *J. Shanxi Univ. Nat. Sci. Ed.* **2010**, *33*, 312–316.
26. Thomasson, A.J. Towards an objective classification of soil structure. *Eur. J. Soil Sci.* **2010**, *29*, 38–46. [CrossRef]
27. Mclean, E.O. Soil pH and lime requirement. In *Methods Soil Analysis Part 2 Chemical Microbiological Properties*; The American Society of Agronomy: Madison, WI, USA, 1982; pp. 199–224.
28. Feng, C.; Yan, M.; Fu, S.; Chen, H.Y.H. Soil Carbon and Nutrient Dynamics Following Cessation of Anthropogenic Disturbances in Degraded Subtropical Forests. *Land Degrad. Dev.* **2017**, *28*, 2457–2467. [CrossRef]
29. Nelson, D.W.; Sommers, L.E.; Sparks, D.L.; Page, A.L.; Helmke, P.A.; Loeppert, R.H.; Soltanpour, P.N.; Tabatabai, M.A.; Johnston, C.T.; Sumner, M.E. Total carbon, organic carbon, and organic matter. *Methods Soil Anal.* **1996**, *9*, 961–1010.
30. Bao, S. *Soil and Agricultural Chemistry Analysis*; China Agriculture Press: Beijing, China, 2000.
31. Jing, Z.; Cheng, J.; Jishuai, S.U.; Bai, Y.U.; Jin, J. Changes in plant community composition and soil properties under 3-decade grazing exclusion in semiarid grassland. *Ecol. Eng.* **2014**, *64*, 171–178. [CrossRef]
32. Zhang, R.; Wang, Z.; Han, G.; Schellenberg, M.P.; Qian, W.; Chen, G. Grazing induced changes in plant diversity is a critical factor controlling grassland productivity in the Desert Steppe, Northern China. *Agric. Ecosyst. Environ.* **2018**, *265*, 73–83. [CrossRef]
33. Davidson, A.; Csillag, F. The influence of vegetation index and spatial resolution on a two-date remote sensing-derived relation to C4 species coverage. *Remote Sens. Environ.* **2001**, *75*, 138–151. [CrossRef]
34. Pinheiro, J.; Bates, D.; DebRoy, S.; Sarkar, D.; Team, R.C. Development Core Team (2011) nlme: Linear and nonlinear mixed effects models. *R Package Version* **2008**, *3*, 1–102.
35. Clarke, K.R. Non-parametric multivariate analyses of changes in community structure. *Aust. J. Ecol.* **1993**, *18*, 117–143. [CrossRef]
36. Fabricius, K.E. Classification and Regression Trees: A Powerful yet Simple Technique for Ecological Data Analysis. *Ecology* **2000**, *81*, 3178–3192.
37. Faith, D.P.; Minchin, P.R.; Belbin, L. Compositional dissimilarity as a robust measure of ecological distance. *Vegetatio* **1987**, *69*, 57–68. [CrossRef]
38. Pardo, I.; Doak, D.F.; Garcíagonzález, R.; Gómez, D.; García, M.B. Long-term response of plant communities to herbivore exclusion at high elevation grasslands. *Biodivers. Conserv.* **2015**, *24*, 3033–3047. [CrossRef]
39. Künnemeyer, R.; Schaare, P.N.; Hanna, M.M. A simple reflectometer for on-farm pasture assessment. *Comput. Electron. Agric.* **2001**, *31*, 125–136. [CrossRef]
40. Yong, Z.; Gao, J.; Ni, S.; Liu, Y.; Jiang, J.; Wei, Y. A spectral reflectance-based approach to quantification of grassland cover from Landsat TM imagery. *Remote Sens. Environ.* **2003**, *87*, 371–375.
41. Huete, A.R. A soil-adjusted vegetation index (SAVI). *Remote Sens. Environ.* **1988**, *25*, 295–309. [CrossRef]
42. Roujean, J.L.; Breon, F. Estimating PAR absorbed by vegetation from bidirectional reflectance measurements. *Remote Sens. Environ.* **1995**, *51*, 375–384. [CrossRef]
43. Cao, S.; Ma, H.; Yuan, W.; Wang, X. Interaction of ecological and social factors affects vegetation recovery in China. *Biol. Conserv.* **2014**, *180*, 270–277. [CrossRef]
44. Gu, Y.; Wylie, B.K.; Bliss, N.B. Mapping grassland productivity with 250-m eMODIS NDVI and SSURGO database over the Greater Platte River Basin, USA. *Ecol. Indic.* **2013**, *24*, 31–36. [CrossRef]

45. Xu, D.Y.; Kang, X.W.; Zhuang, D.F.; Pan, J.J. Multi-scale quantitative assessment of the relative roles of climate change and human activities in desertification—A case study of the Ordos Plateau, China. *J. Arid Environ.* **2010**, *74*, 498–507. [CrossRef]
46. Li, C.; Cao, S. Lack of integrated solutions hinders environmental recovery in China. *Ecol. Eng.* **2013**, *54*, 233–235.
47. He, S.; Richards, K. Impact of Meadow Degradation on Soil Water Status and Pasture Management-A Case Study in Tibet. *Land Degrad. Dev.* **2015**, *26*, 468–479. [CrossRef]